Determination of excited triplet states of dissolved organic matter using chemical probes: a comparative and mechanistic study

Liu, Y.; Cheng, F.; Zhang, T.; Qu, J.; Zhang, Y.; Peijnenburg, W.J.G.M.

Journal of Hazardous Materials 458 (2023) 132011

Contents lists available at ScienceDirect

Journal of Hazardous Materials

journal homepage: www.elsevier.com/locate/jhazmat

Determination of excited triplet states of dissolved organic matter using chemical probes: A comparative and mechanistic study

Yue Liu [a], Fangyuan Cheng [a], Tingting Zhang [a], Jiao Qu [a], Ya-nan Zhang [a,*], Willie J.G.M. Peijnenburg [b,c]

[a] State Environmental Protection Key Laboratory of Wetland Ecology and Vegetation Restoration, School of Environment, Northeast Normal University, Changchun 130117, China
[b] Institute of Environmental Sciences, Leiden University, Leiden, the Netherlands
[c] National Institute of Public Health and the Environment (RIVM), Center for Safety of Substances and Products, Bilthoven, the Netherlands

HIGHLIGHTS

- Differences in determined ^{3}DOM* from isolated DOMs using TMP and HDO were observed.
- The determined excited triplets of selected DOM-analogs are structural dependent.
- Substituents of DOM-analogs could affect the determination of their excited triplets.
- TMP and HDO access different excited triplets and access different pools of ^{3}DOM*.

GRAPHICAL ABSTRACT

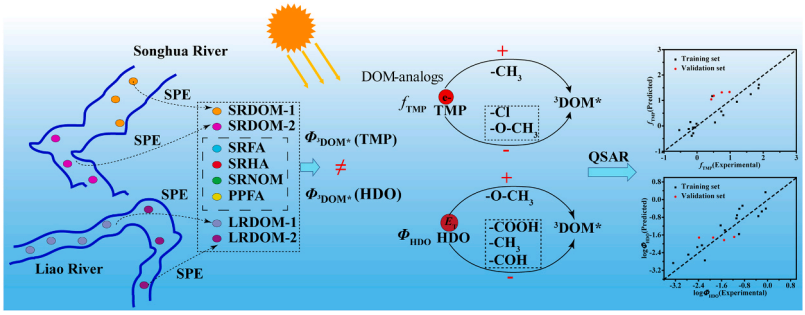

ARTICLE INFO

Editor: Dr. T Meiping

Keywords:
^{3}DOM*
Energy transfer
Electron transfer
Quantitative structure-activity relationship

ABSTRACT

Dissolved organic matter (DOM) plays an important role in the biogeochemical cycle in natural waters. The determination and characterization of the excited triplet state of DOM (^{3}DOM*) have attracted much attention recently. However, the underlying differences of determined ^{3}DOM* through different pathways are not yet fully understood. In this study, the differences and underlying mechanisms of the determined ^{3}DOM* using 2,4-hexadien-1-ol (HDO) through an energy transfer pathway and 2,4,6-trimethylphenol (TMP) through an electron transfer pathway, were investigated. The results showed that the determined quantum yields of ^{3}DOM* ($\Phi_{^3DOM^*}$) for four commercial and four isolated local DOMs are different using HDO ($(0.04 \pm 0.00) \times 10^{-2}$ to $(2.9 \pm 0.17) \times 10^{-2}$)) and TMP ($(0.08 \pm 0.01) \times 10^{-2}$ to $(1.2 \pm 0.17) \times 10^{-2}$), respectively. For 17 DOM-analogs, significant differences were also observed with the quantum yields of their ^{3}DOM* determined using HDO (Φ_{HDO}) and the triplet-state quantum yield coefficients determined using TMP (f_{TMP}). It indicates the different reactivity of TMP and HDO with the excited triplet of the chromophores with different structures within the isolated DOM. Based on the experimental and predicted values of f_{TMP} and Φ_{HDO} for different DOM-analogs, the impact of substituents on differences in ^{3}DOM* values were further revealed. These results demonstrated that the levels of ^{3}DOM* depended on the chemical functionalities present in the DOM-analogs.

* Corresponding author.
E-mail address: zhangyn912@nenu.edu.cn (Y.-n. Zhang).

https://doi.org/10.1016/j.jhazmat.2023.132011
Received 24 April 2023; Received in revised form 16 June 2023; Accepted 5 July 2023
Available online 8 July 2023

1. Introduction

Dissolved organic matter (DOM) can absorb sunlight to generate its excited triplet state (^{3}DOM*) [53]. The ^{3}DOM* is an important photoactive species which can not only directly react with organic pollutants [16,54,67,6], but also sensitize the generation of reactive oxygen species (ROSs), such as singlet oxygen ($^1O_2$) and superoxide anions ($O_2^{\bullet-}$) through energy and electron transfer reactions, respectively ([44,5,9]. These reactive species could significantly affect the environmental behavior of organic pollutants and microorganisms [14,42,43,63]. As reported in previous studies, ^{3}DOM* induced the degradation of cell-free DNA [60], organic pollutants [16,6], cyanotoxins [26], and also could induce the inactivation of microorganisms [59] in natural waters. Thus, considering its important role in the geochemical cycle, the quantitative determination and understanding of the characterization of ^{3}DOM* in natural water are of great significance.

DOM is a heterogeneous mixture that is composed of many small organic molecules with complex structures and a large number of fluorophores, e.g. benzene rings and carbonyl [51,53]. Thus, ^{3}DOM* is not a well-defined species. Instead, it is a mixture of various triplet states [39]. These triplet states are generated from various chromophores with different molecular structures and also with different quantum yields for generation of the excited triplet states. For example, the yields of triplet formation by aromatic ketones are very high [28,47], while coumarins typically have poor triplet yields [27]. Therefore, the contributions of the chromophores with different structures in DOM to the generation of ^{3}DOM* are largely different. This leads to differences in spectral characteristics, photosensitization activity, ability to generate reactive species [15,23,50,57], as well as to difficulties in the quantitative determination of ^{3}DOM* for DOM with different composition as originating from different sources.

The difficulty of quantifying ^{3}DOM* is also attributed to its extremely short lifespan and low steady-state concentration [32]. Chemical probe methods were commonly used and were proven to be a powerful tool for the indirect assessment and quantification of ^{3}DOM* [13,4]. ^{3}DOM* reacts selectively with organic compounds, and its reaction mechanisms mainly include electron transfer and energy transfer pathways [56]. Commonly used probes are thus selected based on their specific redox reaction or energy transfer reaction with ^{3}DOM*. By using chemical probes, the steady-state concentration of ^{3}DOM* ($[^3DOM^*]_{ss}$) in natural waters was estimated to range from 10^{-15} M to 10^{-13} M [56].

Among the chemical probes, 2,4,6-trimethylphenol (TMP), *trans, trans* − 2,4-hexadienoic acid (HDA) and derivatives of HDA (2,4-hexadien-1-ol (HDO) and 2,4-hexadien-1-amine (HDM)) are commonly used for the quantitative determination of ^{3}DOM* [13,19,3,64,7]. TMP reacts with ^{3}DOM* through electron transfer with a reaction rate constant of 3.0×10^9 M^{-1} s^{-1} [3]. HDA, HDO, HDM react with ^{3}DOM* through energy transfer with reaction rate constants of $(0.42 \pm 0.1) \times 10^9$ M^{-1} s^{-1}, $(1.1 \pm 0.1) \times 10^9$ M^{-1} s^{-1}, and $(5.2 \pm 0.4) \times 10^9$ M^{-1} s^{-1}, respectively [64]. In previous studies, little difference in apparent generation quantum yields of ^{3}DOM* (Φ_{3DOM^*}) for DOM, e.g. Pony Lake fulvic acid (PLFA) and, Suwannee River fulvic acid (SRFA), was observed by using the two kinds of chemical probes [34,65]. However, Maizel et al. [36] found that the extracted DOM from Allequash Lake, Big Muskellunge Lake, Sparkling Lake, and Trout Bog had different yields of formation of Φ_{3DOM^*} ($\Phi_{3DOM^*\ (TMP)} > \Phi_{3DOM^*\ (HDA)}$) and $[^3DOM^*]_{ss}$ ($[^3DOM^*]_{ss,TMP} > [^3DOM^*]_{ss,HDA}$). Wasswa et al. [52] also found that there were certain differences in Φ_{3DOM^*} of DOM that was extracted from the Adirondack region of New York, as determined by the two probes.

Besides the quantum yields, the energy (E_T) and redox potentials ($E^{\circ *}$ ($^3S^*/S^{-\bullet}$)) of the determined ^{3}DOM* using the two chemical probes are also different as the triplet states that are generated by various chromophores are different. The ^{3}DOM* is comprised of high-energy triplets (Hi-^{3}DOM*, $E_T \geq 250$ kJ/mol) as well as low-energy triplets (Low-^{3}DOM*, 250 kJ/mol $\geq E_T \geq$ 94 kJ/mol) [56]. Aromatic ketones are reported to have high E_T values [48], and are better candidates for Hi-^{3}DOM* , whereas quinones are most likely not major contributors [45,46,63]. On the contrary, polycyclic aromatic hydrocarbons (PAHs) have relatively low E_T values [21,40]. As to the excited state reduction potential of ^{3}DOM* ($E^{\circ *}$($^3S^*/S^{-\bullet}$)), the compounds with high triplet energies (e.g. ketones) are often powerful oxidants in their triplet states [39], while quinones with low E_T usually have high $E^{\circ *}$ ($^3S^*/S^{-\bullet}$) [20]. Thus, the differences in E_T and $E^{\circ *}$ ($^3S^*/S^{-\bullet}$) of the triplets for different chromophores lead to differences in the determined quantum yields using different chemical probes. The determined ^{3}DOM* using TMP and HDAs respectively are ^{3}DOM* mixtures of different chromophores and also with different photoreactivity. Besides, these probes access different triplet states and thus access different components of ^{3}DOM* . However, explicit interpretation of the ^{3}DOM* determined using TMP (through electron transfer reaction) or HDAs (through energy transfer reaction) is still unclear.

Therefore, this study aims to discuss the inherent relationships between the functional groups of DOM and the electron/energy transfer ability of the generated ^{3}DOM* . Commercial DOM, Suwannee River fulvic acid (SRFA), Suwannee River natural organic matter (SRNOM), Suwannee River humic acid (SRHA) and Pahokee peat fulvic acid (PPFA), and local DOM was that extracted from the Songhua River and the Liao River (SRDOM-1, SRDOM-2, LRDOM-1, and LRDOM-2) were selected as the representative of DOM and 17 small compounds containing chemical substituents that are characteristic parts of DOM were also selected. The Φ_{3DOM^*} for the DOMs and Φ_{HDO}/f_{TMP} for the DOM-ananlogs were measured using the two commonly used chemical probes (HDO and TMP). Analysis and interpretation at the molecular level were performed for understanding the "real" ^{3}DOM* determined using TMP or HDO. Besides, quantitative structure-activity relationship (QSAR) models, which are widely used to correlate molecular structures of organic compounds with their reactivity [61,62], and is used to predict the quantum yield of DOM through different pathways to generate ^{3}DOM* .

2. Materials and methods

2.1. Chemicals

Suwannee River fulvic acid (SRFA), Suwannee River natural organic matter (SRNOM), Suwannee River humic acid (SRHA) and Pahokee peat fulvic acid (PPFA) were obtained from the International Humic Substances Society (IHSS). In addition, four local DOMs were extracted from water samples (10 L) taken from the Songhua River (SRDOM-1 and SRDOM-2) and the Liao River (LRDOM-1 and LRDOM-2), which are located in Jilin, China. Detailed information about the geographic location, morphometry, hydrology of individual rivers, and the method to extract the DOM are summarized in Text S1 in the Supporting Information (SI). These small molecular analogs are with different structures, such as aromatic ketones and quinones, which could represent the main chromophore groups in DOM as proved that DOM contains chromophores such as benzene rings, carbon groups and carboxyl groups. The molecular structures and basic physicochemical parameters of the DOM-analogs and other chemicals used in this study are listed in Text S2 and Table S1 in the SI.

2.2. Light irradiation experiments

Light irradiation experiments were performed with an XPA-7 merry-go-round photochemical reactor (Xujiang Technology Co, Nanjing) equipped with quartz tubes. The solutions were irradiated by a water-refrigerated 500 W medium-pressure mercury lamp, and the temperature was maintained at 25 ± 1 °C by a cooling condenser. The irradiation below 290 nm was filtered with cutoff filters to mimic the UV-A and UV-B portions of sunlight. The light intensity of the Hg lamp used, was measured by a TriOS-RAMSES spectroradiometer (TriOS, GmbH,

Germany) and the result is shown in Fig. S2 in the SI. In the experiments, the DOMs are with initial concentrations of 5 mg-C L^{-1} and the DOM-analogs are with concentrations of 10 mg/L, TMP (0.1 mM) served as the chemical probe for the electron transfer reaction with ^{3}DOM* [22] and HDO (0.01–0.56 mM) served as the chemical probe for the energy transfer reaction with ^{3}DOM* [64]. The solution pH was controlled at 7.0 by preparing phosphate buffer using 0.2 mol/L Na_2HPO_4 and NaH_2PO_4.

2.3. Analytical methods

The UV−vis absorption spectra of the samples were obtained by a UV−vis spectrophotometer (U-2900, Shimadzu Scientific Instruments, Japan). The results are shown in Fig. S3. An Agilent 1260 II HPLC system (Agilent, California, USA) with a UV-Vis detector and an Ultimate TM AQ-C18 column (250 mm × 4.6 mm, 5 mm, Welch Materials, Maryland, USA) was employed for quantification the concentrations of TMP and the isomers of HDO, as detailed in the Table S2. The 3D fluorescence of the DOMs was measured with a fluorescence spectrophotometer (F-2700, Hitachi). The results are shown in Fig. S4.

2.4. Calculation of the quantum yield of generation of ^{3}DOM*

The quantum yield (Φ) is used to calculate the efficiency of photon utilization during photochemical reactions [24]. The quantum yield of ^{3}DOM* was calculated using Eq. (1):

$$\Phi_{^3DOM^*} = \frac{R_{^3DOM^*}}{\sum_\lambda k_{X-a}(\lambda)[X]} \quad (1)$$

where $R_{^3DOM^*}$ represents the formation rate of ^{3}DOM* (mol L^{-1} s^{-1}); $k_{X\text{-}a}$ (λ) is the characteristic light absorption rate of the photosensitizer X (s^{-1}); [X] is the concentration of photosensitizer (mol L^{-1}); the wavelength range is 290–500 nm.

$k_{X\text{-}a}$ (λ) can be defined as follows :

$$k_{X-a}(\lambda) = \frac{I_p \varepsilon_X(\lambda)\left(1 - 10^{-(\alpha(\lambda) + \varepsilon_X(\lambda)[X])z}\right)}{\varepsilon_X(\lambda)[X]z} \quad (2)$$

where I_p is the intensity of incident light (Einstein·s^{-1}·cm^{-2}); $\varepsilon_x(\lambda)$ is the molar absorptivity of the photosensitizer (M^{-1}·cm^{-1}); z is the optical path (cm). The method of measurement is described in Text S3. The detailed methods for detecting $R_{^3DOM^*}$ and [^{3}DOM*]$_{ss}$ using HDO and TMP as the probes are described in Text S3. The quantum yield of the excited triplet state of the selected DOM-analogs determined using HDO was calculated with the same methods.

Due to the reaction rate constant of TMP with differential DOM-analogs are significantly different, the triplet-state quantum yield coefficients for electron transfer (f_{TMP}) was used and calculated using Eq. (3) [34,65]:

$$f_{TMP} = \frac{R_{TMP}}{\sum_\lambda k_{X-a}(\lambda)[X]} \quad (3)$$

where R_{TMP} is the pseudo first-order degradation rate constant of TMP (mol L^{-1} s^{-1})';.

2.5. Establishment, evaluation and validation of QSAR models

The molecular configurations of the target compounds were optimized to obtain the most reasonable geometric structures using the Gaussian 16 program suite [11] with the B3LYP/6–31 +G (d, p) level [1, 29]. The water solvent effect was calculated by means of the integral equation formalism of the polarizable continuum model (IEFPCM) [2, 31]. DRAGON descriptors were calculated using DRAGON software (version 7.0), and constant descriptor values were eliminated. For SRFA with a complex structure, a modeled molecular structure obtained by Leenheer et al. [30] was used.

The $\Phi_{^3DOM^*}$ values of the selected 17 DOM-analogs were log-transformed to obtain a normal-distributed dataset. The data were randomly divided into training sets and verification sets. Then, multiple linear regression (MLR) was used to construct the QSAR model to obtain appropriate molecular structure descriptors and select the best predictive model. This model is used to predict the $\Phi_{^3DOM^*}$ values of other DOM-analogs with various molecular structures. The scientific criteria for evaluating the merits of the QSAR model are shown in Text S4.

3. Results and discussion

3.1. Determination of ^{3}DOM* from DOMs using TMP and HDO

The generation of ^{3}DOM* from SRNOM, SRHA, PPFA, SRFA, and the four local DOMs (SRDOM-1, SRDOM-2, LRDOM-1, and LRDOM-2) was determined using TMP and HDO as the chemical probes. The degradation of TMP was observed in solutions with these DOMs under light irradiation (Fig. S5), indicating the generation of ^{3}DOM* that could react with TMP through electron transfer reactions (The TMP degradation was negligible under dark conditions). The isomerization of HDO in solutions with these DOMs under light irradiation was observed, and the relationships between the sum of formation rates of each isomer (R_p) and different HDO concentrations are shown in Fig. S6. The $\Phi_{^3DOM^*}$, $R_{^3DOM^*}$, and [^{3}DOM*]$_{ss}$ of these DOMs detected with TMP and HDO were calculated, and the results are shown in Table 1 and Table S7.

For the four commercial DOMs, the $\Phi_{^3DOM^*}$ values detected using TMP and HDO are in the range from $(0.08 \pm 0.01) \times 10^{-2}$ to $(0.66 \pm 0.05) \times 10^{-2}$ and $(0.04 \pm 0.00) \times 10^{-2}$ to $(0.41 \pm 0.03) \times 10^{-2}$ respectively, which is in the same order of magnitude with the values reported in previous studies [65,66]. For the four local DOMs, the $\Phi_{^3DOM^*}$ values detected using TMP and HDO are in the range from $(1.0 \pm 0.10) \times 10^{-2}$ to $(1.2 \pm 0.14) \times 10^{-2}$ and $(1.4 \pm 0.10) \times 10^{-2}$ to $(2.9 \pm 0.17) \times 10^{-2}$ respectively, which are significantly higher compared with those of the commercial DOMs. According to the three-dimensional fluorescence diagram (Fig. S4), a major fluorescence peak (peak A in terms of intensity) at Ex/Em = 260/380–460 nm was detected in all the DOMs, indicating a dominance of humic-like substances in these DOMs [8]. The fluorescence intensity (peak A) of commercial DOMs was much lower compared with the fluorescence intensity of the local DOMs, indicating the higher percentage of humic-like materials in the local DOMs [25]. Previous studies have proven that humic-like materials and aromaticity of DOM are positively correlated with the $R_{^3DOM^*}$ and $\Phi_{^3DOM^*}$ values [10,36,49], which is the reason for the higher $\Phi_{^3DOM^*}$ for the four local DOMs.

PPFA has a large number of aromatic carboxylic acid functional groups [55], and the measured values of $\Phi_{^3PPFA^*}$ using TMP ($\Phi_{^3PPFA^*}$(TMP), 0.31×10^{-2}) and HDO ($\Phi_{^3PPFA^*}$(HDO), 0.33×10^{-2}) showed little difference. For SRNOM, $\Phi_{^3SRNOM^*}$(HDO) is twice as high as the $\Phi_{^3SRNOM^*}$(TMP). This indicates that the ^{3}SRNOM* prefers to react with HDO compared with TMP, i.e. most chromophores in SRNOM are with high E_T rather than high $E^{\circ *}$ ($^3S^*/S^{\bullet}$). As reported in previous studies, SRNOM contains highly unsaturated and phenolic groups [37],

Table 1
Φ3DOM* and R3DOM* of DOMs determined using TMP and HDO.

DOMs	$\Phi_{^3DOM^*} \times 10^{-2}$ [a]		$R_{^3DOM^*}$ ($\times 10^{-8}$ M s^{-1})[a]	
	TMP	HDO	TMP	HDO
PPFA	0.31 ± 0.02	0.33 ± 0.02	1.34 ± 0.09	1.48 ± 0.09
SRNOM	0.20 ± 0.02	0.40 ± 0.03	0.46 ± 0.04	0.91 ± 0.06
SRHA	0.08 ± 0.01	0.04 ± 0.00	0.36 ± 0.02	0.17 ± 0.01
SRFA	0.66 ± 0.05	0.41 ± 0.03	3.02 ± 0.20	1.71 ± 0.16
SRDOM-1	1.1 ± 0.13	2.5 ± 0.18	22 ± 2.2	51 ± 3.6
SRDOM-2	1.0 ± 0.10	1.4 ± 0.10	24 ± 2.3	33 ± 2.4
LRDOM-1	1.2 ± 0.14	2.9 ± 0.17	25 ± 3.1	62 ± 3.3
LRDOM-2	1.1 ± 0.11	2.5 ± 0.16	23 ± 2.1	51 ± 3.6

e.g. aromatic carbon and phenolic/carboxylic functional groups [17]. These functional groups are widely known as chromophores with high E_T [39]. On the contrary, the values of Φ_{3SRHA*}(TMP) and Φ_{3SRFA*}(TMP) are higher than those of Φ_{3SRHA*}(HDO) and Φ_{3SRFA*}(HDO). It has been proven that SRHA and SRFA have similar structures. SRHA mainly contained coumaryl, lignin phenylpropane, syringyl, guaiacyl and methoxy groups [18]. In addition to these groups, SRFA also contains formic acid, malonic acid, etc. Haiber et al., ($year$) [18]. These chromophores are widely known to have high values of $E^{\circ *}$ ($^3S^*/S^{-\bullet}$) [33], which leads to the higher Φ_{3SRHA*}(HDO) and Φ_{3SRFA*}(HDO) compared with Φ_{3SRHA*}(TMP) and Φ_{3SRFA*}(TMP).

For the four local DOMs, obvious differences of the Φ_{3DOM*} detected using TMP and HDO were also observed, i.e. Φ_{3DOM*}(HDO) > Φ_{3DOM*}(TMP). These results indicated that most chromophores in the DOM isolated from Songhua River and Liao River are with high E_T instead of high $E^{\circ *}$ ($^3S^*/S^{-\bullet}$). The values of Φ_{3DOM*}(TMP) for the four local DOM showed no obvious difference, and the Φ_{3DOM*}(HDO) of SRDOM-2 is on the lower side compared with other DOMs.

The above results indicated that although in the same order of magnitude, the detected values of Φ_{3DOM*} using TMP and HDO of the DOMs isolated from natural waters, are significantly different from each other. Different structures of the chromophores in different DOMs have been frequently reported [18,58], of which the energy of the triplet and the electron transfer ability are also different ([35]; Was'swa et al., 2020). Thus, it can be concluded that the rate of formation of ^{3}DOM* of a DOM detected using either TMP (via electron transfer reaction) or HDO (via energy transfer reaction) are different in the component (i.e. triplets of different chromophores) from which the triplet state is formed, whereas also the reactivity is different (i.e. different E_T and $E^{\circ *}$ ($^3S^*/S^{-\bullet}$)).

3.2. Determined excited triplet states from DOM-analogs using TMP and HDO

The degradation of TMP was observed in solutions with the DOM-analogs (Fig. S5), indicating that electron transfer reactions occurred between TMP and the excited triplet state of these DOM-analogs. The f_{TMP} were calculated and the results are shown in Table 2. The values of f_{TMP} for the DOM-analogs ranged from (0.29 ± 0.01) to (74 ± 2.4). As can be seen in Table 2, 4-benzoylbenzoic acid, acetophenone, benzophenone, and 3-methoxyacetophenonethe are with relatively high f_{TMP} values compared with the other DOM-analogs. These four compounds are all aromatic ketones, which have been proven to be efficient photosensitizers with high triplet yields and also high values of $E^{\circ *}$ ($^3S^*/S^{-\bullet}$) [39]. This leads to the high value of f_{TMP} measured using TMP. The f_{TMP} values were lower for naphthalene, 2-naphthaldehyde, 1,4-naphthoquinone, 7-hydroxycoumarin, 4-chloro-4′-hydroxybenzophenone, 1,4-benzoquinone, 2-chlorohydroquinone, and trans-cinnamon acid. These compounds are aromatic compounds containing a variety of functional groups, including ketones, quinones, phenols, aldehydes and carboxylic acids.

In solutions with the DOM-analogs under light irradiation, the relationships between the sum of formation rates of each isomer (R_p) and different HDO concentrations are shown in Fig. S6. The Φ_{HDO}, R_{HDO}, and $[HDO]_{ss}$ of the DOM-analogs detected using HDO were calculated and the results are shown in Table 2 and Table S8. The values of Φ_{HDO}, R_{HDO}, and $[HDO]_{ss}$ for the DOM-analogs ranged from (0.05 ± 0.00) × 10^{-2} to (86 ± 1.1) × 10^{-2}, (0.02 ± 0.00) × 10^{-7} M s^{-1} to (36 ± 5.0) × 10^{-7} M s^{-1}, and (0.76 ± 0.00) × 10^{-14} M to (1149 ± 15) × 10^{-14} M, respectively.

As can be seen in Table 2, 3-methoxyacetophenone, naphthalene, 4-benzoylbenzoic acid, and 2-naphthaldehyde are with relatively high Φ_{HDO} values (higher than 47 × 10^{-2}) compared with other DOM-analogs. Among these DOM-analogs, 3-methoxyacetophenone and 4-benzoylbenzoic acid are aromatic ketones, naphthalene belongs to PAHs, and 2-naphthaldehyde is a derivative of PAHs, which have been proven to be efficient photosensitizers with high triplet yields [45,46,63]. Aromatic ketones and polycyclic aromatic hydrocarbons have a high value of Φ_{HDO}, and their ^{3}DOM* have a strong energy transfer ability [57]. Although naphthalene is with high Φ_{HDO}, its R_{HDO} is relatively low due to its low light absorption capacity (Fig. S3). The Φ_{HDO} values were relatively low for 4-chloro-4′-hydroxybenzophenone, trans-cinnamon, gallic acid, duroquinone acid, sodium anthraquinone-2-sulfonate.

3.3. Structural analysis of determined f_{TMP} and Φ_{HDO} for DOM-analogs

The f_{TMP} of DOM-analogs with similar structures, i.e. only with differences in substituents on the benzene ring, are shown in Fig. 1. As can be seen in Fig. 1, the determined f_{TMP} of 3-methoxyacetophenonethe (42 ± 1.5) is lower compared with that of acetophenone (72 ± 2.0), indicating the negative role of methoxy on the generation of their excited triplet state detected through the electron transfer pathway. A methoxy group on the benzene ring has a strong electron donating ability, which could inhibit the electron transfer from TMP to the carbonyl of the excited triplet state of 3-methoxyacetophenonethe. The f_{TMP} of 4-chloro-4′-hydroxybenzophenone (0.56 ± 0.02) and 2-chlorohydroquinone (0.88 ± 0.03) are much lower compared with that of 4-benzoylbenzoic acid (74 ± 2.4), benzophenone (16 ± 0.41), and gallic acid (3.5 ± 0.45), indicating the negative role of chlorine substitution at the phenyl on the generation of the excited triplet state. For the quinones, the f_{TMP} value of duroquinone (2.9 ± 0.19) is much higher than the f_{TMP} values of 1,4-naphthoquinone (0.77 ± 0.02) and 1,4-benzoquinone (0.63 ± 0.01), indicating the positive role of a methyl substituent on the generation of the excited triplet state. This is attributed to the electron withdrawing ability of a methyl group that could increase the reactivity of triplet duroquinone with TMP, and subsequently improved the accuracy of the determination of f_{TMP} using TMP.

The Φ_{HDO} values of the DOM-analogs with similar structures detected using HDO are shown in Fig. 2. As shown in Fig. 2, the determined Φ_{HDO} of 3-methoxyacetophenone ((86 ± 1.1) × 10^{-2}) is higher compared with that of acetophenone ((13 ± 0.46) × 10^{-2}), indicating the positive role of methoxy on the generation of the excited triplet state detected through energy transfer pathway, which is different for the Φ_{HDO} values detected using TMP. The Φ_{HDO} determined using HDO of naphthalene ((83 ± 1.2) × 10^{-2}) is higher compared with that of 2-naphthaldehyde ((47 ± 1.2) × 10^{-2}), indicating the negative role of the aldehyde group on the generation of the excited triplet states or on the energy transfer ability. This is attributed to the electron-withdrawing ability of the aldehyde group, which leads to the decrease of π-electron density on the benzene.

The Φ_{HDO} of benzophenone ((14 ± 0.49) × 10^{-2}) is much lower compared with that of 4-benzoylbenzoic acid ((61 ± 1.6) × 10^{-2}), indicating the negative role of carboxylic acid groups on the generation of the excited triplet state. The Φ_{HDO} value of 1,4-naphthoquinone ((2.3 ± 0.02) × 10^{-2}) and 1,4-benzoquinone ((8.7 ± 0.16) × 10^{-2}) are much higher than that of duroquinone ((0.36 ± 0.00) × 10^{-2}), indicating the negative role of a methyl substituent on the generation of the excited triplet state.

As can be seen in Table 2 the determined f_{TMP} and Φ_{HDO} value for a specific DOM-analog is significantly different using TMP or HDO as the chemical probe. Thus, a comparative analysis was performed with the determined f_{TMP} and Φ_{HDO}. As can be seen in Fig. 3, benzoylbenzoic acid (4-BBA) and 3-methoxyacetophenone (3-MAP) are with both high f_{TMP} and Φ_{HDO} values as determined using TMP and HDO, which have been reported to have high triplet yields [28,47] as well as high triplet energies, which making them strong oxidants of the triplet state [39].

Acetophenone (AP) is with relatively high f_{TMP} and low Φ_{HDO} (Fig. 3). Thus, the excited state of DOM containing such chromophore is susceptible to electron transfer reactions with contaminants rather than energy transfer reactions. Naphthalene (NAP) and 2-naphthaldehyde (2-NAD) are with high Φ_{HDO} and low f_{TMP}. They have diphenyl ring

Table 2
f_{TMP}/Φ_{HDO} of DOM-analogs determined using HDO/TMP.

Compounds	Abbreviations	Structure	f_{TMP} (M^{-1})	$\Phi_{HDO}\times 10^{-2}$
4-Benzoylbenzoic acid	4-BBA	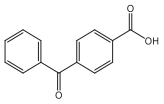	74 ± 2.4	61 ± 1.6
Acetophenone	AP	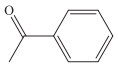	72 ± 2.0	13 ± 0.46
3-Methoxyacetophenone	3-MAP	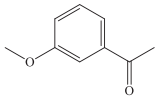	42 ± 1.5	86 ± 1.1
Benzophenone	BP	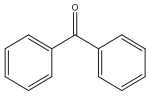	16 ± 0.41	14 ± 0.49
Diacetyl	DC	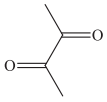	6.2 ± 0.21	10 ± 0.81
4-Chloro-4′-hydroxybenzophenone	44'-HBP	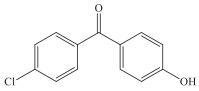	0.56 ± 0.02	0.05 ± 0.00
Sodium anthraquinone-2-sulfonate	AQ2S	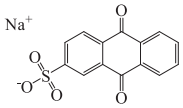	5.4 ± 0.21	0.66 ± 0.04
Duroquinone	DQ	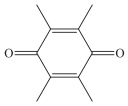	2.9 ± 0.19	0.36 ± 0.00
1,4-Naphthoquinone	NQ	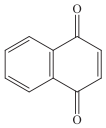	0.77 ± 0.02	2.3 ± 0.02
1,4-Benzoquinone	BQ	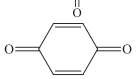	0.63 ± 0.01	8.7 ± 0.16
Riboflavin	RFN	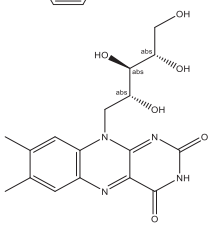	9.6 ± 0.31	1.3 ± 0.01
Naphthalene	NAP	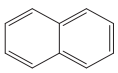	0.96 ± 0.03	83 ± 1.2
2-Naphthaldehyde	2-NAD	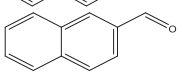	0.76 ± 0.03	47 ± 1.2
7-Hydroxycoumarin	7-HC	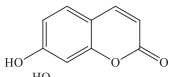	0.29 ± 0.01	3.3 ± 0.08
Gallic acid	GA	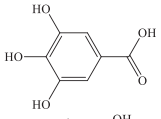	3.5 ± 0.45	0.52 ± 0.00
2-Chlorohydroquinone	2-CDQ	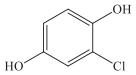	0.88 ± 0.03	10 ± 0.45
Trans-cinnamon acid	*t*-CA	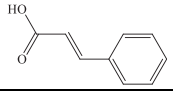	0.69 ± 0.01	0.18 ± 0.00

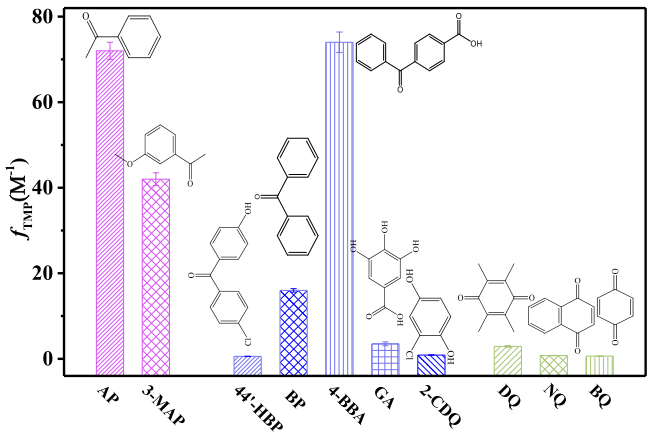

Fig. 1. Plot of the f_{TMP} of similar analogs measured by TMP [The error bars represent the 95% confidence interval ($n = 3$)].

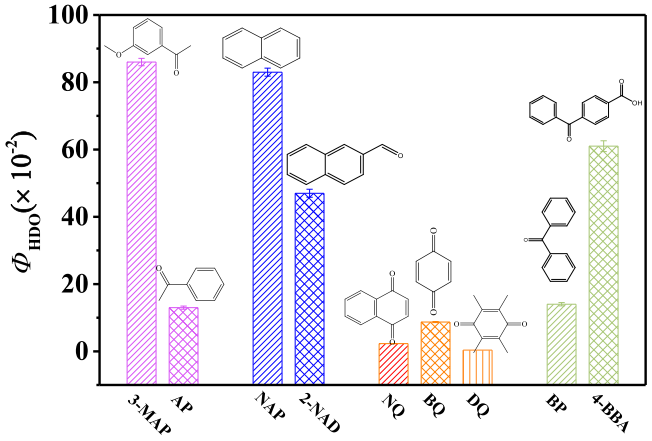

Fig. 2. Plot of the Φ_{HDO} of similar analogs measured by HDO [The error bars represent the 95% confidence interval ($n = 3$)].

structure. Therefore, the excited triplet state of DOM containing above structure is easy to undergo energy transfer reaction with organic pollutants. The remaining DOM-analogs are with both low f_{TMP} and Φ_{HDO} indicating their relatively low contribution to the determined ^{3}DOM* of DOM using TMP as well as HDO.

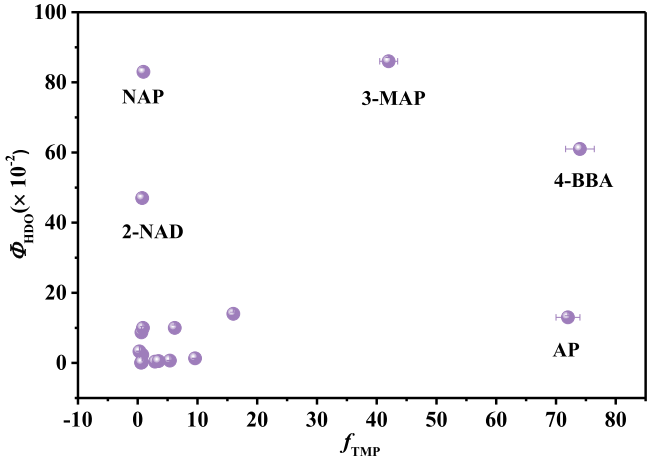

Fig. 3. Determined f_{TMP} and Φ_{HDO} for DOM-analogs using TMP and HDO (NAP: naphthalene, AP: acetophenone, 3-MAP: 3-methoxyacetophenone, 4-BBA: 4-benzoylbenzoic acid, 2-NAD: 2-naphthaldehyde).

3.4. Further mechanism interpretation by constructing QSAR models

As shown above, the Φ_{3DOM^*} of both DOMs and Φ_{HDO} or f_{TMP} of the selected DOM-analogs determined using TMP and HDO are different. Thus, to quickly obtain the Φ_{HDO} or f_{TMP} for various chromophores in DOM as well as to reveal the underlying mechanism for the differences in ^{3}DOM* that were determined using TMP and HDO, two QSAR models were constructed. The QSAR models for f_{TMP} and Φ_{HDO} are shown as equation (4) and equation (5), respectively:

$$\log f_{TMP} = -3.075 + 0.002 \times E_2/E_3 + 3.15 \times SpMin3\_Bh(v) - 0.01 \times P\_VSA\_ppp\_con \quad (4)$$

$n_t = 16$, $R^2_{adj} = 0.815$, $RMSE_t = 0.381$, $F = 9.457$, $Q^2_{LOO} = 0.726$, $p < 0.001$.

$$\log \Phi_{HDO} = -1.698 + 4.147 \times GATS2e + 0.003 \times E_2/E_3 - 15.326 \times HATS1e \quad (5)$$

$n_t = 16$, $R^2_{adj} = 0.811$, $RMSE_t = 0.405$, $F = 17.278$, $Q^2_{LOO} = 0.778$, $p < 0.0001$.

where n_t is the quantity of DOM-analogs in the training set, R^2_{adj} is the adjusted correlation coefficient; $RMSE_t$ is root mean square error, F is the test of variance, Q^2_{LOO} is cross validation coefficient, and p is the significance level of F.

The two QSAR models are with high R^2_{adj} and low $RMSE_t$. This indicates that the developed models have a high goodness of fit. The high values of Q^2_{LOO} showed the good robustness of the constructed models. The distinction between R^2_{adj} and Q^2_{LOO} is less than 0.3, which indicates that the models are not overfitted [12].

There are three molecular descriptors in the two QSAR models respectively. For $QSAR_{TMP}$ model, the descriptor E_2/E_3 (254 nm absorbance divided by that at 365 nm) is an optical physical property parameter, which represents the aromaticity and molecular weight of the DOM-analogs. In the model, $\log f_{TMP}$ values decrease gradually as E_2/E_3 increases. The correlation between E_2/E_3 and the apparent quantum yields of formation of ^{3}DOM* was also reported (Peterson et al., 2012; Bodhipaksha et al., 2015). *SpMin3_Bh(v)* which belongs to the burden eigenvalues descriptors, represents the van der Waals volume of the DOM-analogs. In the model, f_{TMP} values decrease gradually as SpMin3_Bh(v) decreases. *P_VSA_ppp_con* represents the molecular interaction feature shared by a group of active molecules. In the model, f_{TMP} values decrease gradually as *P_VSA_ppp_con* increases. The detailed descriptions of these descriptors and the values for the DOM-analogs are shown in Text S6 and Table S10 in the SI.

For $QSAR_{HDO}$ model, the descriptor E_2/E_3 is also included, which indicates the important role of molecular weight on the formation of the excited triplet state of these DOM-analogs. *GATS2e* shows the dispersion of electronegative atoms at a topological distance equal to 2 bonds in a molecule (Fatemi et al., 2011). In the model, $\log_{3DOM^*}$ values decrease gradually as *GATS2e* decreases, it represents that the higher of *GATS2e* the more appropriate the electron distribution in the DOM molecular structure. So DOM-analogs with strong electronegativity generate ^{3}DOM* when exposed to light. *HATS1e* is also connected to the electronegativity of the DOM-analogs. In the model, $\log_{3DOM^*}$ values decrease gradually as *HATS1e* increases. The detailed descriptions of these descriptors and the values for the DOM-analogs are shown in Text S6 and Table S11 in the SI.

An external verification for the predictive capability of the constructed QSAR models was performed. Besides riboflavin and a commercial DOM (SRFA), two organic pollutants naproxen and fenofibrate acid, which are frequently detected in rivers and structurally similar to the compounds in the training set, were also selected [38,41], of which f_{TMP} and Φ_{HDO} are listed in Table S9. As can be seen in Fig. 4, the predicted $\log \Phi_{HDO}$ and $\log f_{TMP}$ values using the two QSAR models fitted well with the experimental values for both the training set and the validation set. This result demonstrated that the developed QSAR models have a good predictive ability. Besides, the application domains of the two QSAR models are shown in Fig. S9-S12, and a detailed description of these the application domains is provided in Text S7. The

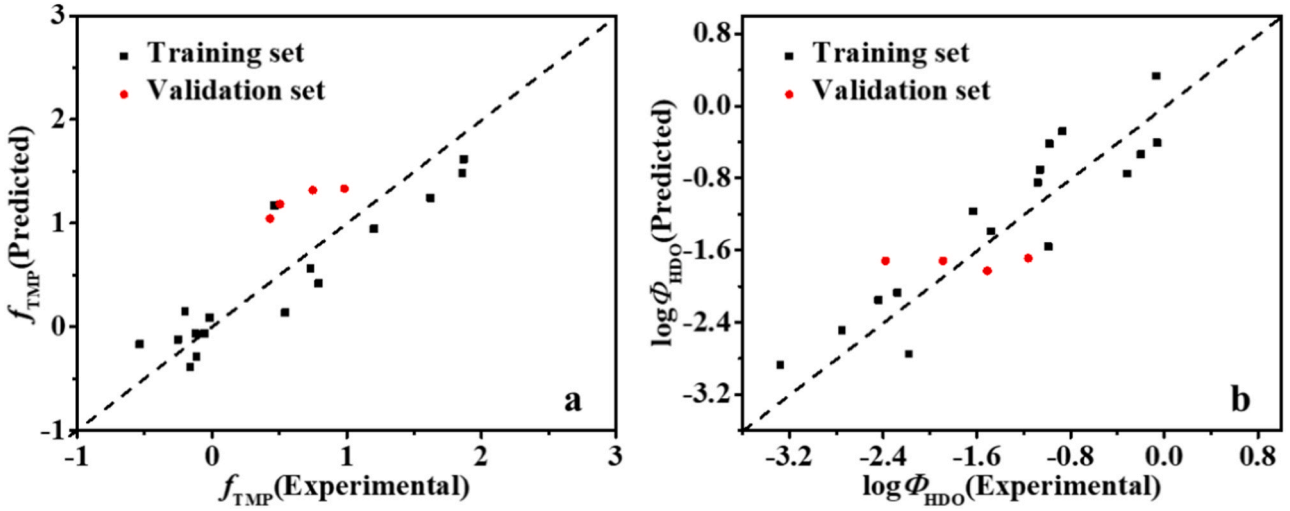

Fig. 4. Plot of predicted versus experimental logf_{TMP} (a) and logΦ_{HDO} (b) values for compounds in training and validation sets.

results showed that the compounds in the training set are of diverse structure and can be used to predict the f_{TMP} and Φ_{HDO} values of various DOM-analogs.

To further investigate the substituent effects on the differences in ^{3}DOM* that were determined using TMP and HDO, more DOM-analogs with different chemical structures were selected, of which logf_{TMP} and logΦ_{HDO} are predicted using the constructed QSAR models. The value of logf_{TMP} and logΦ_{HDO} can be seen in Table S14.

The values of f_{TMP} and Φ_{HDO} for the DOM-analogs with similar structures are shown in Fig. 5. The left side of the red line is the values of f_{TMP} for the DOM-analogs with similar structures, and the right side is Φ_{HDO}. The values of f_{TMP} for naphthalene and its derivatives (part I in Fig. 5) are close. This is due to the low value of the f_{TMP} of these compounds. Thus, the substitution on the naphthalene basic structure showed little effect on the generation of their excited triplet state determined using TMP. Differently, the Φ_{HDO} values of naphthalene and its derivatives are significantly different (part III in Fig. 5). The substitution of a carbonyl increased the Φ_{HDO} while an aldehyde decreased the Φ_{HDO}. These results indicate a negative effect of aldehyde on the energy transfer ability and a positive effect of carbonyl on the energy transfer ability of the excited triplet state of these DOM-analogs.

For the values of f_{TMP} for benzophenone and its derivatives (part II in Fig. 5), the substitution of a carboxyl or hydroxyl chloride atoms or a hydroxyl atoms on the benzophenone greatly affects the values of f_{TMP}. The trend of Φ_{HDO} values of benzophenone and its derivatives (part IV in Fig. 5) are same as f_{TMP} values. Thus, this indicates a positive effect of carboxyl on the electron/energy transfer ability and correspondingly a negative effect of hydroxyl or chloride on the electron/energy transfer ability of the excited triplet state of these DOM-analogs.

4. Conclusions

The determination and characterization of ^{3}DOM* are of great significance for understanding the environmental behavior and effect of DOM in sunlit surface water. HDO and TMP are the mostly used chemical probes for the determination and characterization of ^{3}DOM* . As proven in this study, the determined Φ_{3DOM*}(TMP) and Φ_{3DOM*}(HDO) values of isolated DOMs showed differences when using HDO and TMP through the energy and electron transfer pathway, respectively. For the DOM-analogs with different molecular structures, the values of Φ_{HDO} and f_{TMP} detected using HDO and TMP showed great difference, which indicates that the determined ^{3}DOM* using different probes through different pathways represents different triplet mixtures of chromophores in a DOM, even if the Φ_{3DOM*} has little difference. For the DOM-analogs with similar structures, substituent effects on the determined Φ_{HDO} and f_{TMP} were observed. The methoxy group exhibits for instance a negative effect on the generation of ^{3}DOM* detected through the electron transfer pathway, whereas a methyl group induced a positive effect on the generation of ^{3}DOM* as detected through the electron transfer pathway. Besides, the substitution of a chlorine, aldehyde, or carboxylic acid group could also influence the determined Φ_{HDO} and f_{TMP} values through different pathways. Thus, for the DOM from different water

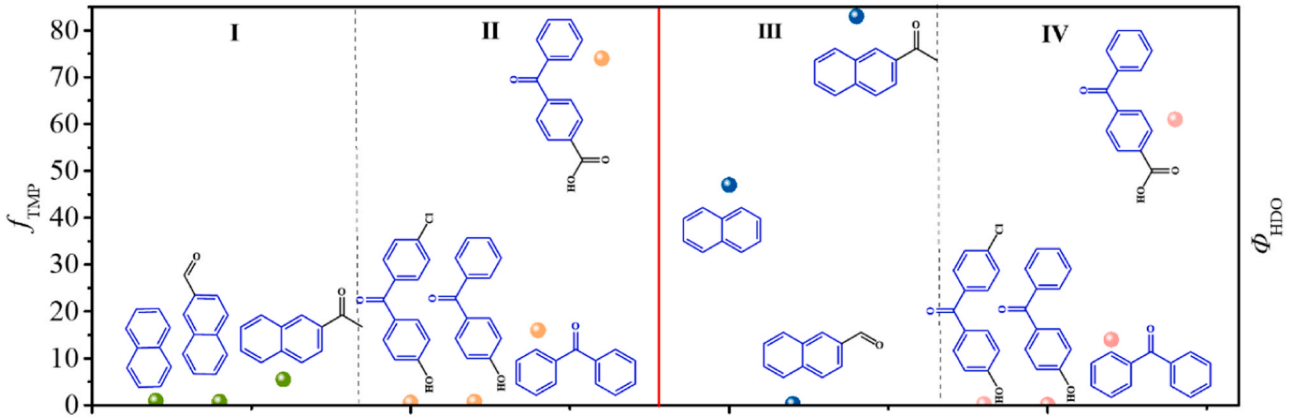

Fig. 5. f_{TMP} and Φ_{HDO} values for other selected DOM-analogs with similar molecular structure.

bodies (fresh water or sea water, river water or lake water, etc.), the choice of different probes to determine their ^{3}DOM* could show certain differences.

The study is useful to further clarify the gap between the identified ^{3}DOM* and the real and complex values in natural waters. Furthermore, it is to be noted that the existing water treatment processes and various emerging advanced oxidation technologies are likely to lead to differentiation in DOM structures, and subsequently lead to differences in the values of ^{3}DOM* as determined by using different chemical probes.

CRediT authorship contribution statement

Yue Liu: Experimental work, Modelling work, Manuscript draft writing and preparation. **Fangyuan Cheng:** Data collection and analysis. **Tingting Zhang:** Supervision, Data curation. **Jiao Qu:** Supervision, Project administration, Funding acquisition. **Ya-nan Zhang:** Conceptualization, Supervision, Writing – review & editing, Funding acquisition. **Willie J.G.M. Peijnenburg:** Writing – review & editing.

Declaration of Competing Interest

The authors declare that they have no known competing financial interests or personal relationships that could have appeared to influence the work reported in this paper.

Data Availability

No data was used for the research described in the article.

Acknowledgments

This work was supported by the National Natural Science Foundation of China (Nos. 22176030, 42130705, 21976027), the Fundamental Research Funds for the Central Universities (No. 2412020FZ015), and the Jilin Province Science and Technology Development Projects (No. 20200301012RQ).

Appendix A. Supporting information

Supplementary data associated with this article can be found in the online version at doi:10.1016/j.jhazmat.2023.132011.

References

[1] Becke, A.D., 1993. Density-functional thermochemistry. III. role Exact Exch J Chem Phys 98 (7), 5648–5652.
[2] Cances, E., Mennucci, B., Tomasi, J., 1997. A new integral equation formalism for the polarizable continuum model: theoretical background and applications to isotropic and anisotropic dielectrics. J Chem Phys 107 (8), 3032–3041.
[3] Canonica, S., Hellrung, B., Wirz, J., 2000. Oxidation of phenols by triplet aromatic ketones in aqueous solution. J Phys Chem A 104, 1226–1232.
[4] Cawley, K.M., Hakala, J.A., Chin, Y.P., 2009. Evaluating the triplet state photoreactivity of dissolved organic matter isolated by chromatography and ultrafiltration using an alkylphenol probe molecule. Limnol Oceano: Methods 7, 391–398.
[5] Chen, L., Tang, X., Shen, C., Chen, C., Chen, Y., 2012. Photosensitized degradation of 2,4′,5-trichlorobiphenyl (PCB 31) by dissolved organic matter. J Hazard Mater 201, 1–6.
[6] Cheng, F., He, J., Li, C., Lu, Y., Zhang, Y.-N., Qu, J., 2021. Photo-induced degradation and toxicity change of decabromobiphenyl ethers (BDE-209) in water: effects of dissolved organic matter and halide ions. J Hazard Mater 416, 125842.
[7] Chin, Y.P., Miller, P.L., Zeng, L.K., Cawley, K., Weavers, L.K., 2004. Photosensitized degradation of bisphenol A by dissolved organic matter. Environ Sci Technol 38 (22), 5888–5894.
[8] Coble, P.G., 1996. Characterization of marine and terrestrial DOM in sea water using excitation–emission matrix spectroscopy. Mar Chem 51 (4), 325–346.
[9] Dalrymple, R.M., Carfagno, A.K., Sharpless, C.M., 2010. Correlations between dissolved organic matter optical properties and quantum yields of singlet oxygen and hydrogen peroxide. Environ Sci Technol 44 (15), 5824–5829.
[10] De Laurentiis, E., Minella, M., Maurino, V., Minero, C., Brigante, M., Mailhot, G., et al., 2012. Photochemical production of organic matter triplet states in water samples from mountain lakes, located below or above the tree line. Chemosphere 88 (10), 1208–1213.
[11] Frisch, M.J. , Trucks, G.W. , Schlegel, H.B. , Scuseria, G.E. , Robb, M.A. , Cheeseman, J.R. , et al. , 2016. Gaussian 16, revision b.01, gaussian, inc., wallingford ct.
[12] Golbraikh, A., Tropsha, A., 2002. Beware of q^2! J Mol Graph Model 20 (4), 269–276.
[13] Grebel, J.E., Pignatello, J.J., Mitch, W.A., 2011. Sorbic acid as a quantitative probe for the formation, scavenging and steady-state concentrations of the triplet-excited state of organic compounds. Water Res 45 (19), 6535–6544.
[14] Guerard, J.J., Chin, Y.P., Mash, H., Hadad, C.M., 2009. Photochemical fate of sulfadimethoxine in aquaculture waters. Environ Sci Technol 43 (22), 8587–8592.
[15] Guerard, J.J., Miller, P.L., Trouts, T.D., Chin, Y., 2009. The role of fulvic acid composition in the photosensitized degradation of aquatic contaminants. Aquat Sci 71, 160–169.
[16] Guo, Z., Wang, J., Chen, X., Cui, F., Wang, T., Zhou, C., et al., 2021. Photochemistry of dissolved organic matter extracted from coastal seawater: excited triplet-states and contents of phenolic moieties. Water Res 188, 116568.
[17] Gutierrez, L., Nguyen, T.H., 2013. Interactions between rotavirus and natural organic matter isolates with different physicochemical characteristics. Water Res 29 (47), 14460–14468.
[18] Haiber, S., Herzog, H., Burbah, P., Gosciniak, B., Lambert, J., 2001. Two-dimensional NMR studies of size fractionated Suwannee River Fulvic and Humic Acid reference. Environ Sci Technol 35 (21), 4289–4294.
[19] Halladja, S., Halle, A., Aguer, J.P., Boulkamh, A., Richard, C., 2007. Inhihition of humic substances mediated photooxygenation of furfuryl alcohol by 2,4,6-trimethylphenol. Evidence for reactivity of the phenol with humic triplet excited states. Environ Sci Technol 41 (17), 6066–6073.
[20] Hayano, S., Fujihira, M., 1971. The effect of water on the reduction potentials of some aromatic compounds in the DMF–water system. B Chem Soc Jpn 44 (8), 2051–2055.
[21] Herkstroeter, J.S., Hammond, G.S., 1966. Mechanisms of photochemical reactions in solution. xxxix. 1 study of energy transfer by kinetic spectrophotometry. J Am Chem Soc 88 (21), 4769–4777.
[22] Jin, W., Cheng, F., Liu, Y., Yang, H., Zhou, Y., Qu, J., et al., 2022. Insights into generation mechanisms of halogen radicals from excited triplet state of dissolved organic matter. Sci Total Environ 834, 155280.
[23] Kellerman, A.M., Guillemette, F., Podgorski, D.C., Aiken, G.R., Butler, K.D., Spencer, R.G.M., 2018. Unifying concepts linking dissolved organic matter composition to persistence in aquatic ecosystems. Environ Sci Technol 52 (5), 2538–2548.
[24] Kishino, M., Okami, N., Takahashi, M., Ichimura, S.-E., 1986. Light utilization efficiency and quantum yield of phytoplankton in a thermally stratified sea1. Limnol Oceano 31 (3), 557–566.
[25] Korak, J.A., Dotson, A.D., Summers, R.S., Rosario-Ortiz, F.L., 2014. Critical analysis of commonly used fluorescence metrics to characterize dissolved organic matter. Water Res 49, 327–338.
[26] Kurtz, T., Zeng, T., Rosario-Ortiz, F.L., 2021. Photodegradation of cyanotoxins in surface waters. Water Res 192, 116804.
[27] Kuznetsova, N.A., Kaliya, O.L., 1992. The photochemistry of coumarins. Russ Chem Rev 61 (7), 683.
[28] Lamola, A.A., Hammond, G.S., 1965. Mechanisms of photochemical reactions in solution. XXXIII. Inter Crossing Effic J Chem Phys 43 (6), 2129.
[29] Lee, C., Yang, W., Parr, R.G., 1988. Development of the Colle-Salvetti correlation-energy formula into a functional of the electron density. Phys Rev B Condens Matter 37 (2), 785–789.
[30] Leenheer, J.A., McKnight, D.M., Thurman, E.M., Maccarthy, P., 1989. Structural components and proposed structural models of fulvic acid from the Suwannee River in Humic substances in the Suwannee River, Georgia: Interactions, properties, and proposed structures. U S Geol Surv.
[31] Li, C., Wei, G., Chen, J., Zhao, Y., Zhang, Y.-N., Su, L., et al., 2018. Aqueous •OH radical reaction rate constants for organophosphorus flame retardants and plasticizers: Experimental and modeling studies. Environ Sci Technol 52 (5), 2790–2799.
[32] Li, Y., Wei, X., Chen, J., Xie, H., Zhang, Y.-N., 2015. Photodegradation mechanism of sulfonamides with excited triplet state dissolved organic matter: a case of sulfadiazine with 4-carboxybenzophenone as a proxy. J Hazard Mater 290, 9–15.
[33] Litter, M.I., Navío, J.A., 1994. Comparison of the photocatalytic efficiency of TiO_2, iron oxides and mixed Ti(IV)-Fe(III) oxides: photodegradation of oligocarboxylic acids. J Photo Photobio A 84 (2), 183–193.
[34] Maizel, A.C., Remucal, C.K., 2017. Molecular composition and photochemical reactivity of size-fractionated dissolved organic matter. Environ Sci Technol 51 (4), 2113–2123.
[35] Maizel, A.C., Remucal, C.K., 2017. The effect of probe choice and solution conditions on the apparent photoreactivity of dissolved organic matter. Environ Sci: Process Impacts 19 (8), 1040–1050.
[36] Maizel, A.C., Li, J., Remucal, C.K., 2017. Relationships between dissolved organic matter composition and photochemistry in lakes of diverse trophic status. Environ Sci Technol 51 (17), 9624–9632.
[37] Maqbool, T., Sun, M., Chen, L., Zhang, Z., 2022. Molecular-level characterization of natural organic matter in the reactive electrochemical ceramic membrane system for drinking water treatment using FT-ICR MS. Sci Total Environ 846, 157531.
[38] Martínez Bueno, J.M., Gomez, M.J., Herrera, S., Hernando, M.D., Agüera, A., Fernández-Alba, A.R., 2012. Occurrence and persistence of organic emerging

contaminants and priority pollutants in five sewage treatment plants of Spain: two years pilot survey monitoring. Environ Pollut 164, 267–273.
[39] McNeill, K., Canonica, S., 2016. Triplet state dissolved organic matter in aquatic photochemistry: reaction mechanisms, substrate scope, and photophysical properties. Environ Sci: Process Impacts 18, 1381–1399.
[40] Merkel, P.B., Dinnocenzo, J.P., 2008. Thermodynamic energies of donor and acceptor triplet states. J Photo Photo A 193 (2), 110–121.
[41] Palanivel, B., Hossain, M.S., Macadangdang Jr, R.R., Ayappan, C., Krishnan, V., Marnadu, R., et al., 2021. Activation of persulfate for improved naproxen degradation using $FeCo_2O_4$@g-C_3N_4 heterojunction photocatalysts. ACS Omega 6 (50), 34563–34571.
[42] Parker, K.M., Mitch, W.A., 2016. Halogen radicals contribute to photooxidation in coastal and estuarine waters. Proc Natl Acad Sci USA 113 (21), 5868–5873.
[43] Rosado-Lausell, S.L., Wang, H., Gutiérrez, L., Romero-Maraccini, O.C., Niu, X., Gin, K.Y.H., et al., 2013. Roles of singlet oxygen and triplet excited state of dissolved organic matter formed by different organic matters in bacteriophage MS2 inactivation. Water Res 47 (14), 4869–4879.
[44] Rosario-Ortiz, F.L., Canonica, S., 2016. Probe compounds to assess the photochemical activity of dissolved organic matter. Environ Sci Technol 50 (23), 12532–12547.
[45] Sharpless, C.M., 2012. Lifetimes of triplet dissolved natural organic matter (DOM) and the effect of $NaBH_4$ reduction on singlet oxygen quantum yields: implications for DOM photophysics. Environ Sci Technol 46 (8), 4466–4473.
[46] Sharpless, C.M., Aeschbacher, M., Page, S.E., Wenk, J., Sander, M., McNeill, K., 2014. Photooxidation-Induced changes in optical, electrochemical, and photochemical properties of humic substances. Environ Sci Technol 48 (5), 2688–2696.
[47] Wagner, P.J., Hammond, G.S., 1966. Mechanisms of photochemical reactions in solution. XXXVIII.[1] Quenching of the Type II photoelimination reaction. J Am Chem Soc 88 (6), 1245–1251.
[48] Wagner, P.J., Truman, R.J., Puchalski, A.E., Wake, R., 1986. Extent of charge transfer in the photoreduction of phenyl ketones by alkylbenzenes. J Am Chem Soc 108 (24), 7727–7738.
[49] Wang, J., Chen, J., Qiao, X., Wang, Y., Cai, X., Zhou, C., et al., 2018. DOM from mariculture ponds exhibits higher reactivity on photodegradation of sulfonamide antibiotics than from offshore seawaters. Water Res 144, 365–372.
[50] Wang, J., Chen, J., Qiao, X., Zhang, Y.-N., Uddin, M., Guo, Z., 2019. Disparate effects of DOM extracted from coastal seawaters and freshwaters on photodegradation of 2,4-dihydroxybenzophenone. Water Res 151, 280–287.
[51] Wang, W., He, C., Gao, Y., Zhang, Y., Shi, Q., 2019. Isolation and characterization of hydrophilic dissolved organic matter in waters by ion exchange solid phase extraction followed by high resolution mass spectrometry. Environ Chem Lett 17, 1857–1866.
[52] Wasswa, J., Driscoll, C.T., Zeng, T., 2020. Photochemical characterization of surface waters from lakes in the Adirondack region of New York. Environ Sci Technol 54 (17), 10654–10667.
[53] Wenk, J., Eustis, S.N., McNeill, K., Canonica, S., 2013. Quenching of excited triplet states by dissolved natural organic matter. Environ Sci Technol 47 (22), 12802–12810.
[54] Xu, H., Cooper, W.J., Jung, J., Song, W., 2011. Photosensitized degradation of amoxicillin in natural organic matter isolate solutions. Water Res 45, 632–638.
[55] Yao, Y., Wang, X., Yang, Y., Shen, T., Wang, C., Tang, Y., et al., 2019. Molecular composition of size-fractionated fulvic acid-like substances extracted from spent cooking liquor and its relationship with biological activity. Environ Sci Technol 53 (24), 14752–14760.
[56] Zepp, R.G., Schlotzhauer, P.F., Sink, R., 1985. Photosensitized transformations involving electronic energy transfer in natural waters: role of humic substances. Environ Sci Technol 19 (1), 74–81.
[57] Zhang, D., Yan, S., Song, W., 2014. Photochemically induced formation of reactive oxygen species (ROS) from effluent organic matter. Environ Sci Technol 48 (21), 12645–12653.
[58] Zhang, F., Li, X., Duan, L., Zhang, H., Gu, W., Yang, X., et al., 2021. Effect of different DOM components on arsenate complexation in natural water. Environ Pollut 270, 116221.
[59] Zhang, T., Chen, F., Yang, H., Zhu, B., Li, C., Zhang, Y.-N., et al., 2022. Photochemical degradation pathways of cell-free antibiotic resistance genes in water under simulated sunlight irradiation: Experimental and quantum chemical studies. Chemosphere 302, 134879.
[60] Zhang, Y.-N., Zhang, T., Liu, H., Qu, J., Li, C., Chen, J., et al., 2020. Simulated sunlight-induced inactivation of tetracycline resistant bacteria and effects of dissolved organic matter. Water Res 185, 116241.
[61] Zhao, J., Zhou, Y., Li, C., Xie, Q., Chen, J., Chen, G., et al., 2020. Development of a quantitative structure-activity relationship model for mechanistic interpretation and quantum yield prediction of singlet oxygen generation from dissolved organic matter. Sci Total Environ 712, 136450.
[62] Zhong, S., Hu, J., Yu, X., Zhang, H., 2021. Molecular image-convolutional neural network (CNN) assisted QSAR models for predicting contaminant reactivity toward OH radicals: transfer learning, data augmentation and model interpretation. Chem Eng J 408 (15), 127998.
[63] Zhou, H., Lian, L., Yan, S., Song, W., 2017. Insights into the photo-induced formation of reactive intermediates from effluent organic matter: The role of chemical constituents. Water Res 112, 120–128.
[64] Zhou, H., Yan, S., Ma, J., Lian, L., Song, W., 2017. Development of novel chemical probes for examining triplet natural organic matter under solar illumination. Environ Sci Technol 51 (19), 11066–11074.
[65] Zhou, H.X., Yan, S.W., Lian, L.S., Song, W.H., 2019. Triplet-state photochemistry of dissolved organic matter: triplet-state energy distribution and surface electric charge conditions. Environ Sci Technol 53 (5), 2482–2490.
[66] Zhou, Y., Cheng, F., He, D., Zhang, Y.-N., Qu, J., Yang, X., et al., 2021. Effect of UV/chlorine treatment on photophysical and photochemical properties of dissolved organic matter. Water Res 192, 116857.
[67] Zhou, Z., Chen, B., Qu, X., Fu, H., Zhu, D., 2018. Dissolved black carbon as an efficient sensitizer in the photochemical transformation of 17β-Estradiol in aqueous solution. Environ Sci Technol 52, 10391–10399.